Supporting Information

Unique Structural Relaxations and Molecular Conformations of Porphyra-334 at the Excited State

Makoto Hatakeyama,[*ab] Kenichi Koizumi,[b] Mauro Boero,[e] Katsuyuki Nobusada,[cd] Hirokazu Hori,[f] Taku Misonou,[f] Takao Kobayashi,[g] Shinichiro Nakamura[*bh]

[a] Faculty of Pharmaceutical Sciences, Sanyo-Onoda City University, 1-1-1 Daigakudori, Sanyo-Onoda, Yamaguchi 756-0884, Japan

[b] RIKEN Cluster for Science, Technology and Innovation Hub, 2-1 Hirosawa, Wako, Saitama 351-0198, Japan

[c] Department of Theoretical and Computational Molecular Science, Institute for Molecular Science, Myodaiji, Okazaki, 444-8585, Japan

[d] Elements Strategy Initiative for Catalysts and Batteries (ESICB), Kyoto University, Katsura, Kyoto 615-8520, Japan

[e] University of Strasbourg, Institut de Physique et Chimie des Matériaux de Strasbourg (IPCMS), CNRS, UMR 7504, 23 rue du Loess, F-67034, Strasbourg, France

[f] Graduate School of University of Yamanashi 4-4-37, Takeda, Kofu, Yamanashi, 400-8510, Japan

[g] Mitsubishi Chemical Corporation, MCC-Group Science and Technology Research Center Inc., 1000 Kamoshida-cho, Aoba-ku, Yokohama 227-8502, Japan

[h] Computational Chemistry Applications Unit, Advanced Center for Computing and Communication, RIKEN, 2-1, Hirosawa, Wako, Saitama, 351-0198, Japan

Supporting Information

S1. Franck-Condon excitation energy of the deprotonated/protonated porphyra-334

The Franck-Condon (FK) excitation energies of the deprotonated-anion and protonated-cation forms of porphyra-334 were analyzed to provide a comparison with the neutral forms. The structures of these charged forms are schematically shown in Figure S1. FK energies are summarized in Table S1. We remark that the deprotonated-anion forms having one CN double bond (**A**-**D** of Figure S1) show FK energies of the spin-singlet first excited state (S_1) above 90 kcal/mol, hence similar to the neutral less polar forms (**A** and **B** of Figure 1 in the main text). Conversely, some structures having one CN double bond present S_1 FK energies below 90 kcal/mol, reflecting the non-planar structural distortion of the S_0 optimized geometry due to the intra-molecular hydrogen bonding interaction(s). Other deprotonated anion forms having no CN double bond (**E** and **F** of Figure S1) are characterized by S_1 FK energies below 85 kcal/mol in many structures, thus being similar to the neutral zwitter-ion forms (**C** and **D** of Figure 1 in the main text). Some structures of the deprotonated-anion form **F** could not be analyzed because these revert spontaneously to the more stable forms (**A**-**D** of Figure S1) during the structural optimization through an intra-molecular H^+ transfer from the COOH groups to the non-protonated CN groups.

By considering the Gibbs free energies, the form **D** turns out to be the energetically more favorable deprotonated-anion form in aqueous solution. Thus, the most probable deprotonated-anion form, characterized by an S_1 FK energy below 85 kcal/mol, is similar to the zwitter-ion forms, and it can be identified as the most probable neutral forms in water. An analogous trend was found also in the protonated form **G** (see Figure S1 and Table S1). Therefore, the S_1 FK energies of the charged forms turn out to be nearly comparable with those of the neutral forms at least in solution.

S2. Mulliken's population analysis on porphyra-334

The atomic charges of porphyra-334 were quantified in terms of Mulliken's population analysis on the S_0 and S_1 states at both of the S_0 and S_1 optimized structures within a DFT(wB97XD)/6-31G(d) approach (Table S2). In Table S2, summarizing this analysis, each atom is numbered as shown in Figure S2. The results of Table S2 were calculated at the lowest

energy structure of the S_0 state in the zwitter-ion form **C** (corresponding to the sample (1) of Table S3). At the S_0 optimized structure of the zwitter-ion form, the S_0 state showed a positive charge on the carbon atoms of the CN groups (C4 and C5 in Figure S2 and Table S2) rather than the central carbon atom of the cyclohexene ring (C6 in Figure S2 and Table S2). This trend is due to the partial shift of the π electrons from the cyclohexene ring to the protonated CN group as shown in terms of highest occupied π orbital of the S_0 state in Figures 2e, 5a and 5b of the main text. The partial π electron shift was induced by the change from the less-polar form to the zwitter-ion form. Furthermore, the π electron shift is enhanced in the S_1 state at the S_0 optimized structure, and this is reflected by the changes of the atomic charges at the relevant three carbon atoms (C4, C5 and C6 of Table S2). The π electron shift is more evident in the S_1 state at the S_1 optimized structure, because the carbon atom of the bending threonine-arm comes closer to the charge neutral conditions in this situation (C5 of Table S2). The π electron shift at the S_1 optimized structure is also evidenced by the S_1-S_0 electron density difference ($\Delta\rho$) which indicates a density decrease at the cyclohexene ring (cyan-colored lobe in Figure S3) and a corresponding increase at the CN group of the bending threonine-arm (orange-colored lobe in Figure S3).

S3. Quantum chemical calculations on porphyra-334

Multi-configurational SCF calculations were done on the configuration of the zwitter-ion form **C** labeled as sample (1) (see Table S3 and S11) by using the complete active space SCF method with six active electrons and five active orbitals (i.e. CASSCF(6,5)). The five active orbitals were chosen by considering the S_0 state at the planar S_0 optimized structure and the S_1 state at the non-planar S_1 optimized structure. The active orbitals of the S_0 state were chosen according to the following criteria; (i) totally bonding orbital consisting of the five 2p atomic orbitals at the two CN bonds and the cyclohexene ring, (ii) non-bonding orbital consisting of the two π orbitals at the CN bonds, (iii) bonding orbital having a π orbital at the cyclohexene ring and a π^* orbitals at the two CN bonds, (iv) non-bonding orbital consisting of the two π^* orbitals at the CN bonds and (v) totally anti-bonding orbital consisting of the five 2p atomic orbitals at the two CN bonds and the cyclohexene ring (Figure S4). The S_1 state carries the five active orbitals at the non-planar S_1 optimized structure as follows; (I) lone-pair orbital at the N atom in the glycine-arm, (II) π orbital of the CN bond in the bending threonine-arm, (III) π orbital of the

C-C bond in the cyclohexene ring, (IV) π^* orbital in the bending threonine-arm and (V) π^* orbital in the cyclohexene ring (Figure S5). Both of the S_0 active orbitals (Figure S4) and the S_1 active orbitals (Figure S5) consist of the five 2p orbitals perpendicular or tilted from the C-N and C-C bonds of porphyra-334. In this way, both of the S_0 and S_1 states are accessible for a direct analysis in terms of CASSCF(6,5) calculations.

Within this same CASSCF(6,5) approach, the S_1 and S_0 energies were analyzed (see Figure S6) in particular along the N_{thr}-C-CH_2-C dihedral angle. The results turn out to be numerically identical to those provided by TDDFT calculation (Figure 4 in the main text). In the energy refinement, the CASSCF(6,5) calculation was done at the TDDFT optimized structures without any additional CASSCF(6,5) structural optimization. For the CASSCF(6,5) calculation, the average over the S_1 and S_0 states was used. As a result, the CASSCF(6,5) calculation show an S_1-S_0 energy gap reduction along the N_{thr}-C-CH_2-C dihedral change, in a way analogous to the TDDFT calculations. We can also remark that CASSCF(6,5) calculations suggest the presence of the S_1 stationary point at a dihedral angle N_{thr}-C-CH_2-C of about 80º, consistently with TDDFT results. The presence of this point is further confirmed by CIS calculations. Moreover, the CASSCF(6,5) calculation also indicates a multi-configurational character to be partially associated with porphyra-334, despite such a character is not treated in the TDDFT calculation. In practice, the CASSCF(6,5) indicates the S_0 state to have a 94% contribution (i.e., 0.97 squared) from the Hartree-Fock configuration state function (CSF). A further sophisticated method like CASPT2 (complete active space second-order perturbation theory) would be needed in investigating a situation where the S_0 and S_1 states are extremely close to each other or actually crossing like a conical intersection.

An additional analysis of the S_1 and S_0 energies was done by Symmetry Adopted Cluster-Configuration Interaction (SAC-CI) calculations (Figure S7). This choice was driven by the fact that the SAC-CI approach provides the best agreement for the S_1 ($\pi\pi^*$) Franck-Condon excitation energy with the experimental absorption maximum (see Table 1 in the main text), at variance with other theoretical approaches (TDDFT, CASSCF(6,5) and CIS). This energy refinement at the SAC-CI level was done fixing the geometry to the TDDFT optimized structures. The results of these SAC-CI calculation show the following three trends (Figure S7); (i) an S_1-S_0 energy gap reduction along the N_{thr}-C-CH_2-C dihedral angle, (ii) an early contact between the S_1 and S_0 energies at a value of the dihedral N_{th}-C-CH_2-C angle of about 110º and

(iii) a non-smooth change of the S_1 energy upon the use of the TDDFT optimized structures. The trend (iii) is particularly evident at ~150° where the S_0 energy increases abruptly. Such a non-smooth trend can be found also with other Haree-Fock based method, e.g. CIS. The feature labeled as (ii) above can be ascribed to the the SAC-CI calculations of the S_1 ($\pi\pi^*$) Franck-Condon excitation energy, which is indeed smaller than analogous results obtained within the TDDFT and CASSCF(6,5) approaches. Then, the trend (ii) implied the possibility of an S_1-S_0 energy crossing. So far, the trend (ii) seems to be inconsistent with the experimental excited-state lifetime (~ 0.4 ns) which is longer than a typical lifetime of an excited state having a conical intersection (of the order of the ps or fs).

Moreover, the S_1 energy was also investigated in terms of its parameter dependence at TDDFT(ωB97XD) calculation. In practice, the S_1 energy was analyzed in varying the value of the parameter ω of ωB97XD functional. The parameter ω was varied from the original value (0.2), which was used in investigating the results shown in the text, to 0.0, 0.1 0.3, 0.4. The resulting S_1 energies were summarized in Table S4. Then, it was found that the S_1 excitation energy is varied in the range of about 2-10 [kcal/mol] by changing the ω parameter in the range stated above. Although such a change was realized, it did not change a trend that the experimental S_1 energy (85.6 [kcal/mol]) is more close to the results of the zwitter-ion forms (**C**, **D**) rather than those of the less-polar forms (**A**, **B**). Therefore, we confirm that the TDDFT(ωB97XD) result of the S_1 energy depends on the parameter ω in quantitative degree rather than in qualitative degree.

The S_1 state was also analyzed in terms of its component of the orbital excitations at TDDFT(ωB97XD) calculation with the parameter ω as 0.2 (Table S5). Table S5 shows that the S_1 state is dominated by the excitation from the highest occupied π orbital to the lowest unoccupied π^* orbital with its large excitation coefficient. The highest occupied π orbital is shown in Figure 2 and 5 of the text, and it corresponds to the highest occupied Kohn-Sham orbital of the S_0 state. Similarly, the lowest unoccupied π^* orbital cis shown in the Figure 2 and 6 of the text, and it corresponds to the lowest unoccupied Kohn-Sham orbital of the S_0 state at DFT(ωB97XD) calculation. These Kohn-Sham orbitals are also analyzed in comparing them to the natural transition orbitals (NTOs).[1] NTOs were calculated for the S_1 state at both of the S_0 optimized structure (Figure S8) and the S_1 optimized structure (Figure S9). As a result, the highest occupied NTO for the S_1 state at the S_0 optimized structure (Figure S8b) was identified

to be analogous to the highest occupied Kohn-Sham orbital of the S_0 state at the S_0 optimized structures (Figure 5ab of the main text) which contributes to the S_1 state as the highest occupied π orbital as stated above. Similarly, the lowest unoccupied NTO for the S_1 state at the S_0 optimized structure (Figure S8c), the highest occupied NTO for the S_1 state at the S_1 optimized structure (Figure S9b) and the lowest unoccupied NTO for the S_1 state at the S_1 optimized structure (Figure S9c) were identified to be analogous to the lowest unoccupied Kohn-Sham orbital of the S_0 state at the S_0 optimized structure (Figure 6ab), highest occupied Kohn-Sham orbital of the S_0 state at the S_1 optimized structure (Figure 5cd) and lowest unoccupied Kohn-Sham orbital of the S_0 state at the S_1 optimized structure (Figure 6cd), respectively. Therefore, it is confirmed that the S_1 state can be well represented by both Kohn-Sham orbitals and NTOs.

4. Triplet states on porphyra-334

The triplet states were analyzed to investigate the possibility of a triplet-singlet intersystem crossing after photoexcitation for both of the less-polar forms (**A** and **B** of Figure 1 in the text) and the zwitter-ion forms (**C** and **D** of Figure 1 in the text). For instance, among the frontier orbitals of the less-polar form **A** (Figure S10), the nitrogen lone-pair (n) orbital of the CN_{thr} double bond is the second highest occupied orbital (see (b) of Figure S10) in the energy spectrum. Then, the N lone-pair orbital is involved in the excitation to the lowest unoccupied π^* orbital ((d) of Figure S10). The resulting spin-triplet $n\pi^*$ state appears as the second triplet state (T_2) in-between the T_1 ($\pi\pi^*$) and S_1 ($\pi\pi^*$) states. The Franck-Condon excitation energies of the T_1 and T_2 states are reported in Table S6 and can be compared directly with the S_1 energy of Table S3. Among the various Franck-Condon structures, analyzed to account for the various orientations of the terminal residues, some structures showed the T_2 ($n\pi^*$) state energy just below the S_1 ($\pi\pi^*$) state. Hence, these structures of the less-polar forms are prone to have an intersystem crossing possibility after photoexcitation to the S_1 ($\pi\pi^*$) state.

The zwitter-ion forms (see Figure 1 of the text), at variance with the less-polar form, present an N-H bonding orbital instead of a lone pair. Such a change is due to a proton transfer from the COOH group to the non-protonated CN group. As a complementary information, we remark that among the frontier-orbitals of the zwitter-ion form **C** (Figure S11), the N-H bonding orbital is the 48th occupied orbital according to the ordering of our energy spectrum (see (a) of Figure S11) instead of second highest occupied orbital. Thus, the N-H bonding orbital can

hardly participate to the triplet state in the moderate energy region. At the zwitter-ion form, the spin-triplet first (T_1) state is the $\pi\pi^*$ state, and the spin-triplet second (T_2) state is the CT state corresponding to the electron transfer from the COO^- group to the π^* orbital at the CN group, being similar to the case of the spin-singlet excited states.

The energy levels of the triplet states were also analyzed along its relaxation coordinate of the S_1 state (i.e. N_{thr}-C-CH_2-C dihedral angle), as shown in Figure S12. The energy levels were analyzed at the sample (1) of the zwitter-ion form **C** (see also Table S11, S12). The energy level of the lowest triplet state (T_1), which was characterized as the $\pi\pi^*$ state, became close to the energy levels of the singlet $\pi\pi^*$ state (S_1) and singlet ground state (S_0) in accordance with the change of the S_1 relaxation coordinate. Meanwhile, the energy level of the second lowest triplet state (T_2) did not become close to those of the singlet states even after the change of the S_1 relaxation coordinate. As a result, it is found that only the T_1 state has a possibility of the intersystem crossing with the S_1 state during the S_1 relaxation process.

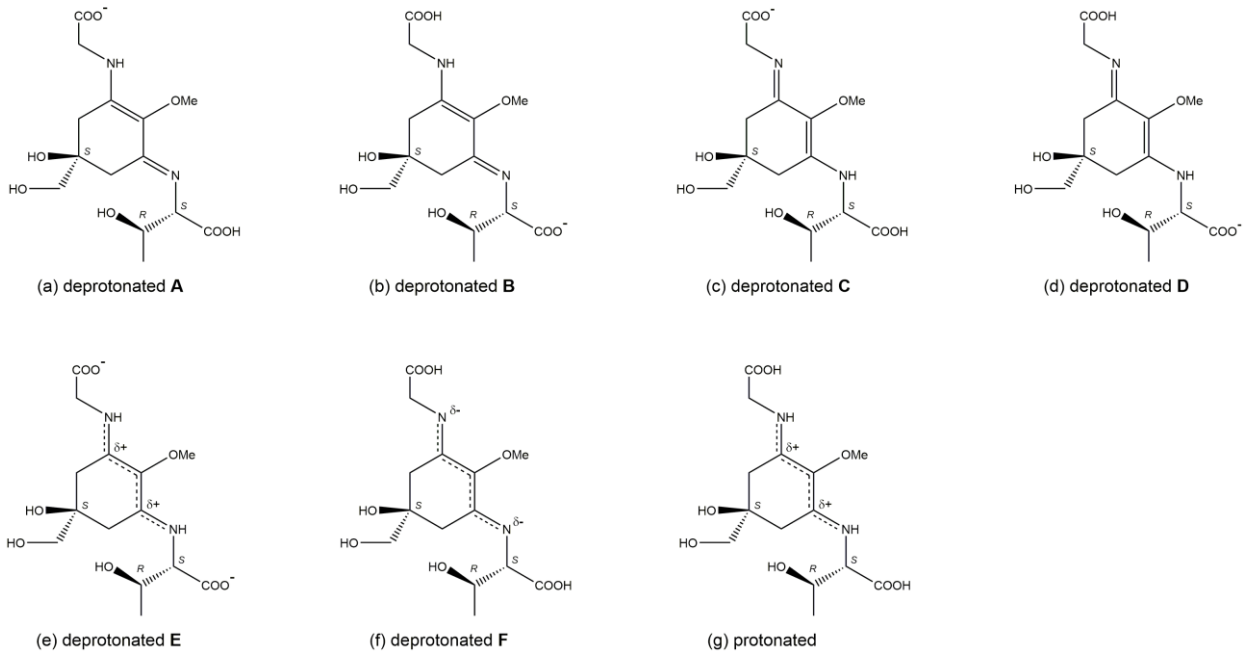

Figure S1. Schematic representation of the deprotonated/protonated forms of porphyra-334 in the spin-singlet ground state (S_0).

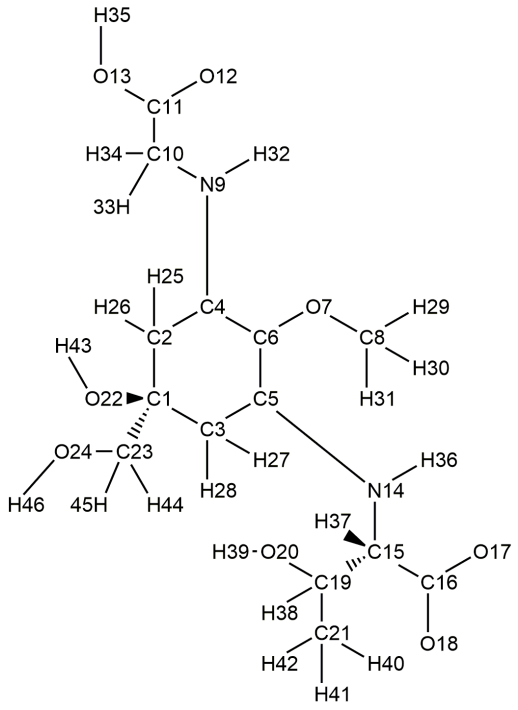

Figure S2. Atomic numberings on the sample (1) of the zwitter-ion form **C** (see Table S3 and S10).

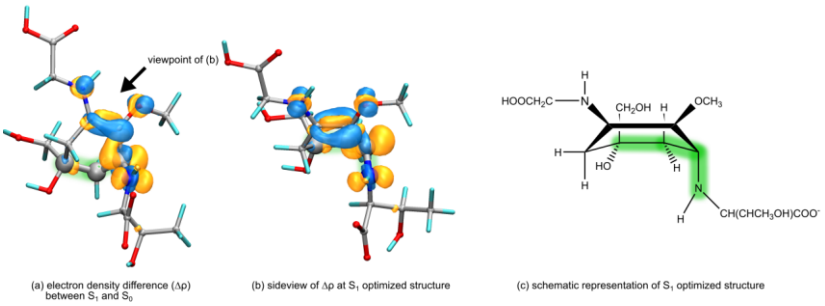

Figure S3. (a) Electron density difference (Δρ) between S_0 and S_1 states of the zwitter-ion form **C** at the S_1 optimized structure, (b) side view of Δρ between S_0 and S_1 states of the zwitter-ion form **C** at the S_1 optimized structure and (c) schematic representation of the S_1 optimized structure.

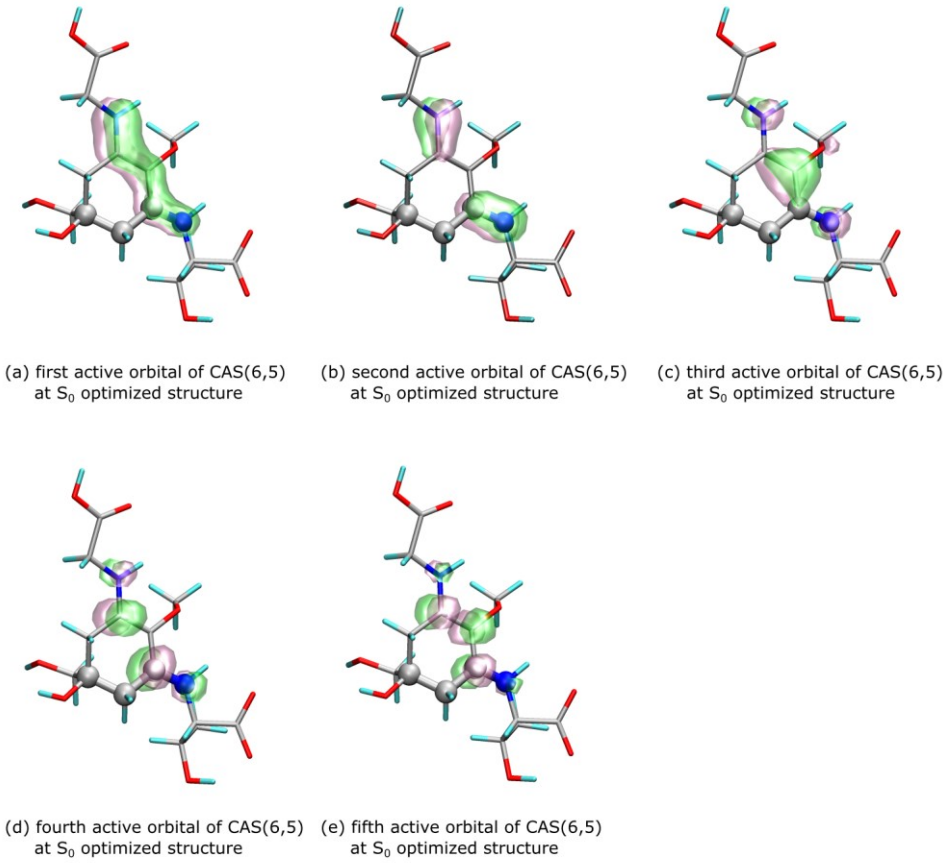

Figure S4. (a) first active orbital of CASSCF(6,5) calculation at the S_0 optimized structure, (b) second active orbital of CASSCF(6,5) calculation at the S_0 optimized structure, (c) third active orbital of CASSCF(6,5) calculation at the S_0 optimized structure, (d) fourth active orbital of CASSCF(6,5) calculation at the S_0 optimized structure and (e) fifth active orbital of CASSCF(6,5) calculation at the S_0 optimized structure.

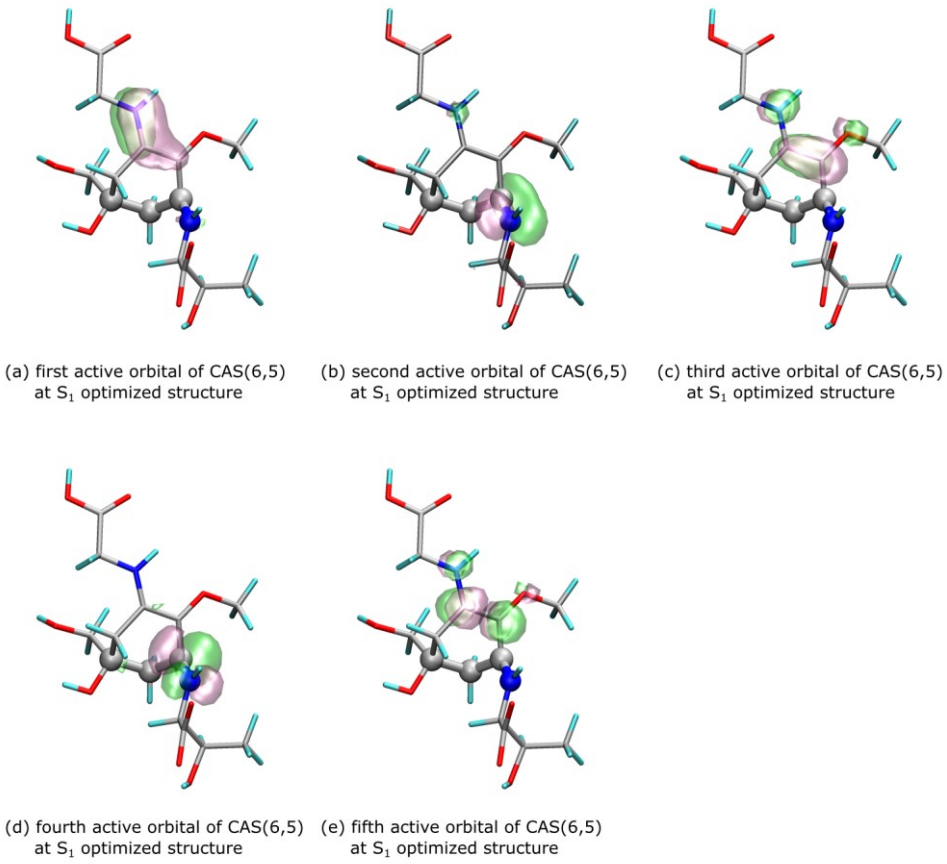

Figure S5. (a) first active orbital of CASSCF(6,5) calculation at the S_1 optimized structure, (b) second active orbital of CASSCF(6,5) calculation at the S_1 optimized structure, (c) third active orbital of CASSCF(6,5) calculation at the S_1 optimized structure, (d) fourth active orbital of CASSCF(6,5) calculation at the S_1 optimized structure and (e) fifth active orbital of CASSCF(6,5) calculation at the S_1 optimized structure.

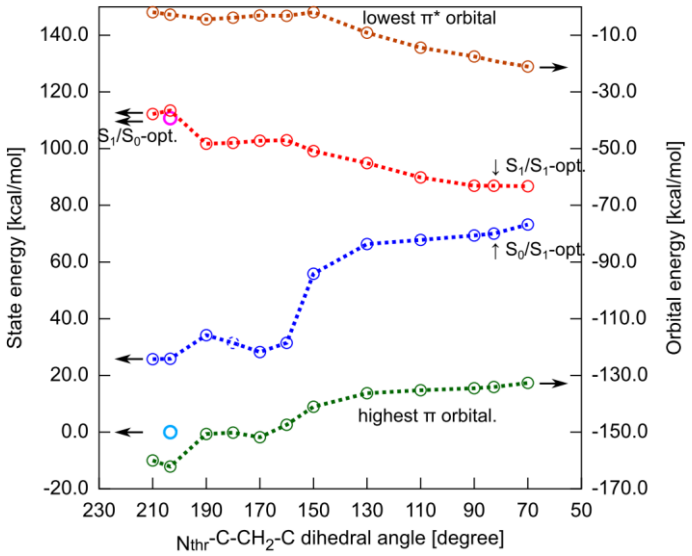

Figure S6. State energies and orbital energies obtained by CAS(6,5) calculation at the DFT/TDDFT optimized structures of the zwitter-ion form **C** (cyan; S_0 energy at the S_0 optimized structure, pink; S_1 energy at the S_0 optimized structure, red; S_1 energy at the (constrained) S_1 optimized structure, blue; S_0 energy at the (constrained) S_1 optimized structure, green; highest π orbital energy at the (constrained) S_1 optimized structure, orange; lowest π* orbital energy at the (constrained) S_1 optimized structure).

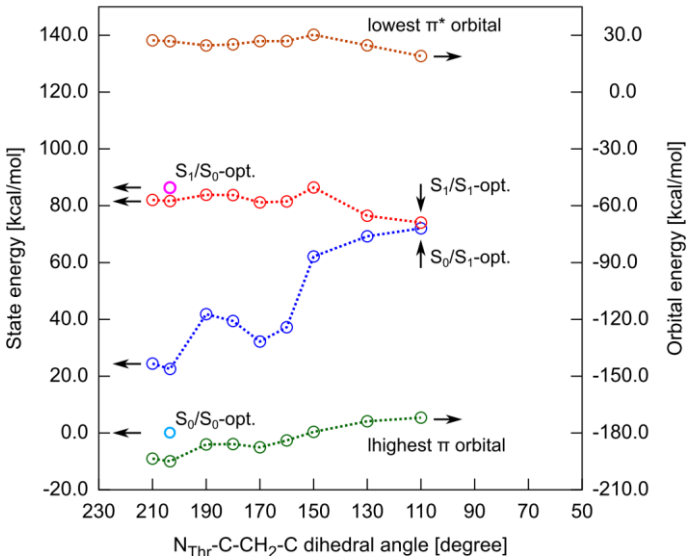

Figure S7. State energies by SAC-CI and Hartree-Fock orbital energies at the DFT/TDDFT optimized structures of the zwitter-ion form **C** (cyan; S_0 energy at the S_0 optimized structure, pink; S_1 energy at the S_0 optimized structure, red; S_1 energy at the (constrained) S_1 optimized structure, blue; S_0 energy at the (constrained) S_1 optimized structure, green; highest π orbital energy at the (constrained) S_1 optimized structure, orange; lowest π* orbital energy at the (constrained) S_1 optimized structure).

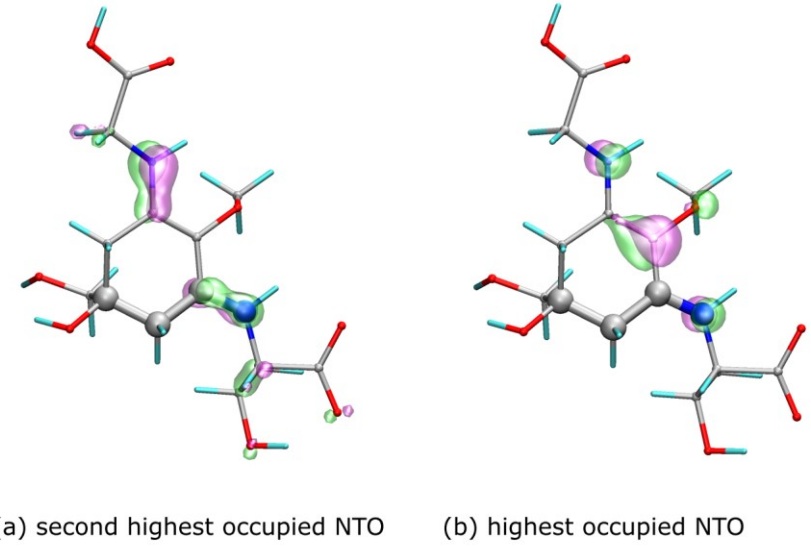

(a) second highest occupied NTO (b) highest occupied NTO

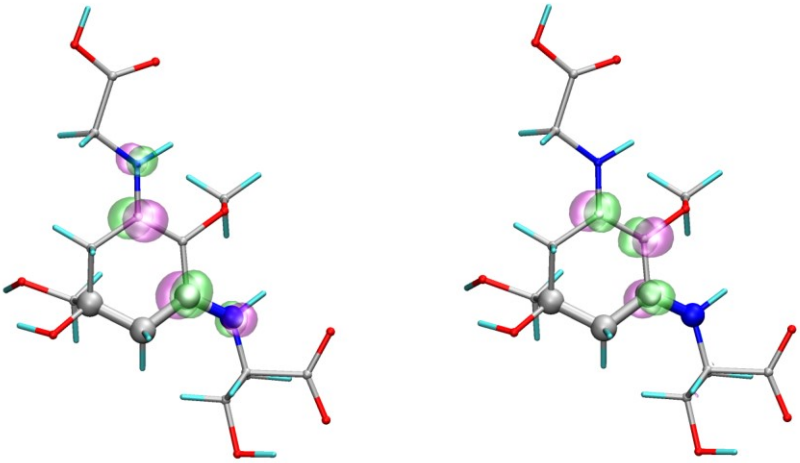

(d) lowest unoccupied NTO (e) second lowest unoccupied NTO

Figure S8. Natural transition orbitals (NTOs) for the S_1 state at the S_0 optimized structure; (a) second highest occupied NTO, (b) highest occupied NTO, (c) lowest unoccupied NTO and (d) second lowest NTO.

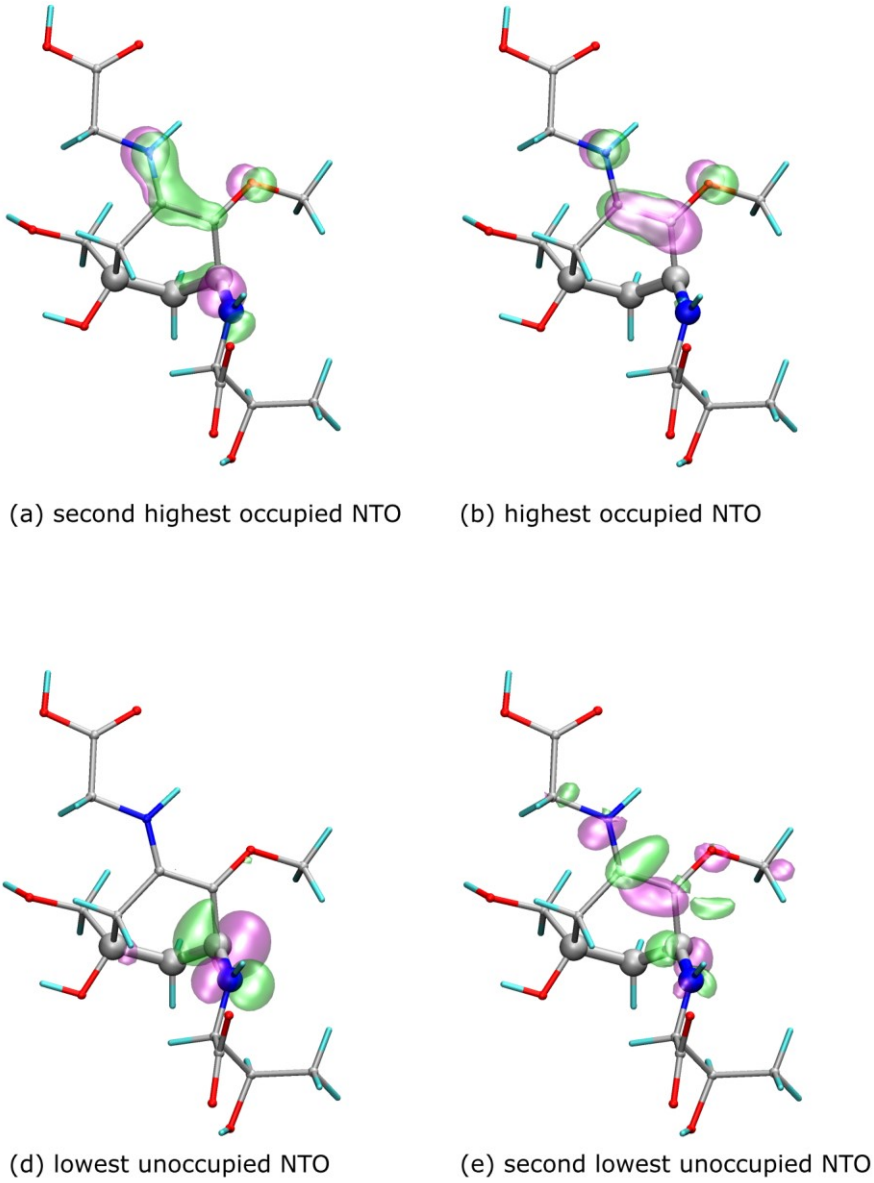

Figure S9. Natural transition orbitals (NTOs) for the S_1 state at the S_1 optimized structure; (a) second highest occupied NTO, (b) highest occupied NTO, (c) lowest unoccupied NTO and (d) second lowest NTO.

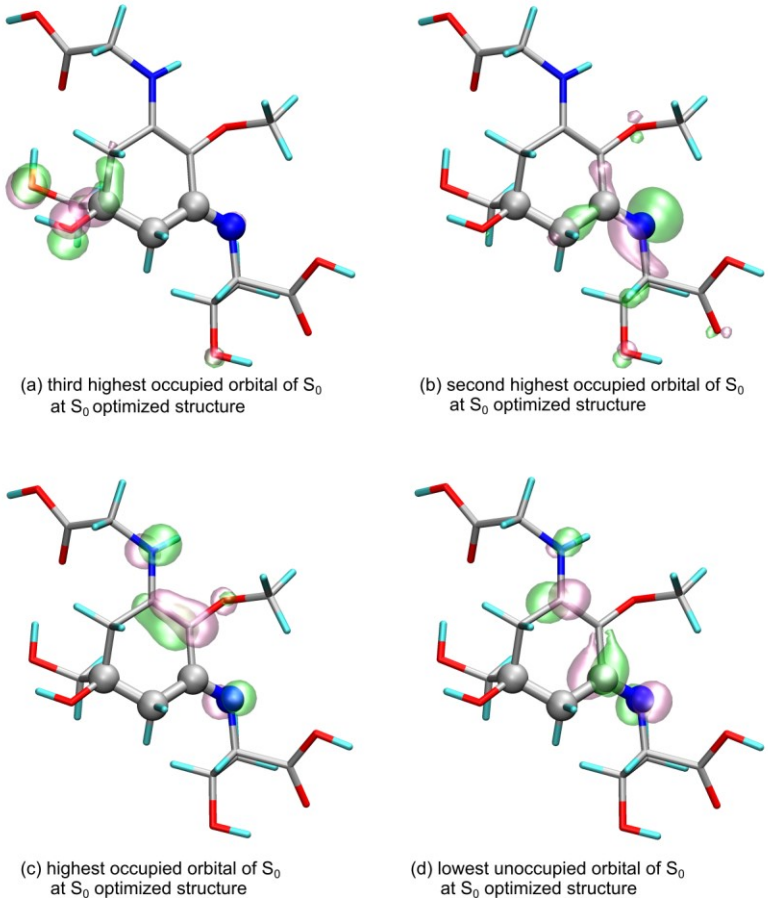

Figure S10. (a) third highest occupied Kohn-Sham orbital of the S_0 state at the S_0 optimized structure of less-polar form **A**, (b) second highest occupied Kohn-Sham orbital of the S_0 state at the S_0 optimized structure of less-polar form **A**, (c) highest occupied Kohn-Sham orbital of the S_0 state at the S_0 optimized structure of less-polar form **A** and (d) lowest unoccupied Kohn-Sham orbital of the S_0 state at the S_0 optimized structure of less-polar form **A**.

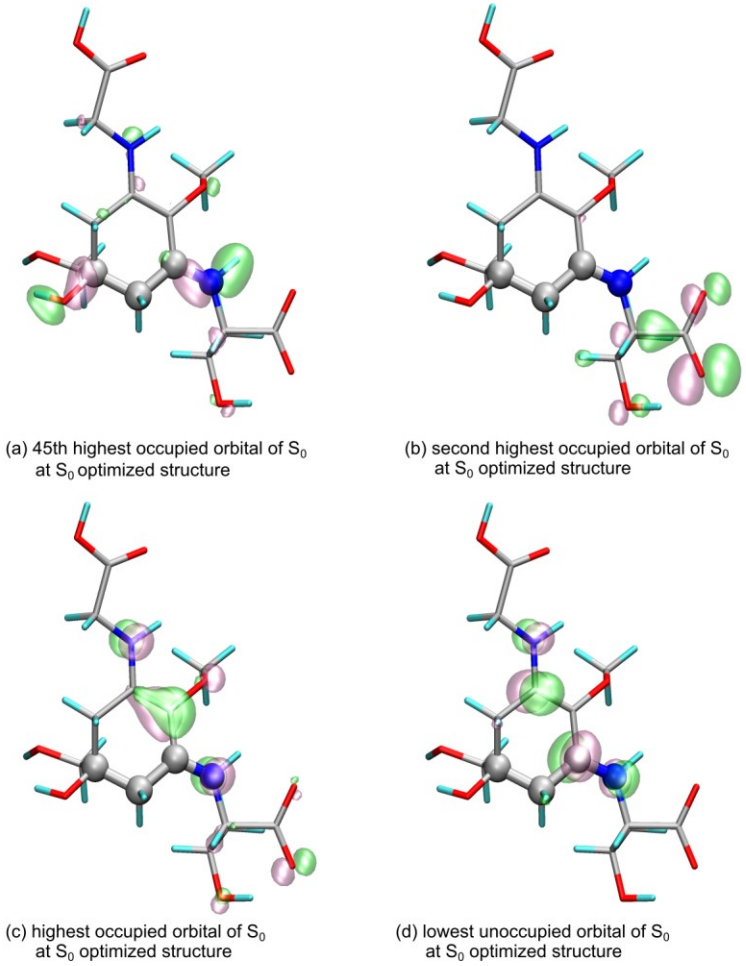

Figure S11. (a) 48th highest occupied Kohn-Sham orbital of the S_0 state at the S_0 optimized structure of zwitter-ion form **C**, (b) second highest occupied Kohn-Sham orbital of the S_0 state at the S_0 optimized structure of zwitter-ion form **C**, (c) highest occupied Kohn-Sham orbital of the S_0 state at the S_0 optimized structure of zwitter-ion form **C** and (d) lowest unoccupied Kohn-Sham orbital of the S_0 state at the S_0 optimized structure of zwitter-ion form **C**.

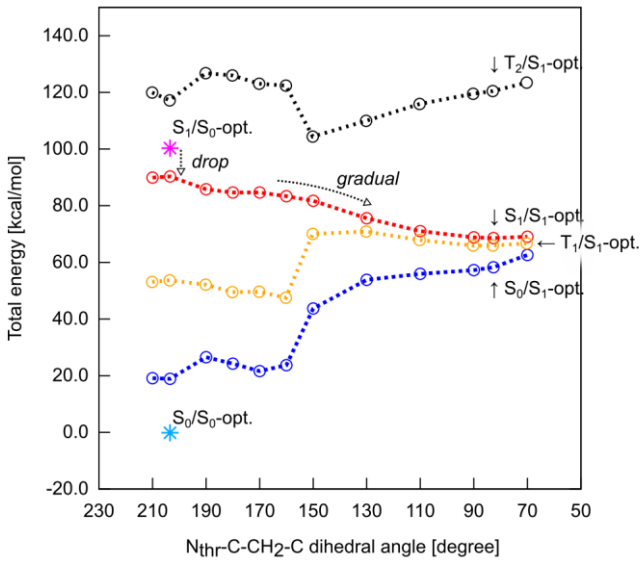

Figure S12. State energies and orbital energies obtained by DFT/TDDFT calculation at the DFT/TDDFT optimized structures of the zwitter-ion form **C** (cyan; S_0 energy at the S_0 optimized structure, pink; S_1 energy at the S_0 optimized structure, red; S_1 energy at the (constrained) S_1 optimized structure, blue; S_0 energy at the (constrained) S_1 optimized structure, orange; T_1 energy at the (constrained) S_1 optimized structure, black; T_2 energy at the (constrained) S_1 optimized structure).

Table S1. Frank-Condon excitation energies [eV] of the spin-singlet first excited states for the deprotonated forms (**A**-**F**, see Figure S1) and protonated form (**G** of Figure S1) of porphyra-334.

form	geometry sample	Gibbs free energy [a.u]	FC [kcal/mol] by SAC-CI
A	1	-1256.87970	91.827841
	2	-1256.86228	95.729294
	3	-1256.86372	93.874949
	4	-1256.86746	97.423667
	5	-1256.86366	93.501714
	6	-1256.86984	89.753406
	7	-1256.87575	87.586014
	8	-1256.87388	88.258137
	9	-1256.87183	88.843714
	10	-1256.87601	86.368971
B	1	-1256.871782	106.458214
	2	-1256.863034	104.598219
	3	-1256.859351	108.850169
	4	-1256.858309	108.268789
	5	-1256.861843	109.907726
	6	-1256.878496	103.997791
	7	-1256.879111	109.166329
	8	-1256.865755	109.833355
	9	-1256.863515	105.942695
	10	-1256.871384	103.942953
C	1	-1256.86129	106.674798
	2	-1256.85925	107.017178
	3	-1256.85302	108.101139
	4	-1256.85700	105.328131
	5	-1256.85438	106.851142
	6	-1256.85890	108.521510
	7	-1256.85601	107.967319
	8	-1256.85475	109.185492

	9	-1256.85790	108.368388
	10	-1256.85737	108.332045
D	1	-1256.87194	96.984133
	2	-1256.87144	98.720938
	3	-1256.86295	102.133969
	4	-1256.87183	93.367017
	5	-1256.86391	100.545005
	6	-1256.88331	99.340483
	7	-1256.87505	98.838709
	8	-1256.86992	94.943252
	9	-1256.88319	99.351575
	10	-1256.87155	96.229823
E	1	-1256.89532	86.038813
	2	-1256.88704	82.787506
	3	-1256.89019	85.007476
	4	-1256.88947	82.522679
	5	-1256.88152	86.697976
	6	-1256.89353	83.892522
	7	-1256.89552	85.385231
	8	-1256.89914	80.152746
	9	-1256.89713	79.832228
	10	-1256.89222	81.566750
F	1	-1256.83311	76.887834
	2	-1256.83241	80.368547
	3	-1256.82499	77.733626
	4	-1256.83048	79.997388
	5	-1256.82313	76.664792
	6	-1256.83336	78.200971
	7	-	-
	8	-	-
	9	-1256.83674	77.379785

	10	-1256.83386	73.410165
G	1	-1257.798514	82.264631
	2	-1257.792082	80.897164
	3	-1257.797033	83.307383
	4	-1257.793888	78.564036
	5	-1257.786995	80.429427
	6	-1257.793494	80.533776
	7	-1257.793666	81.326321
	8	-1257.798539	79.276330
	9	-1257.798256	80.842003
	10	-1257.797519	81.491988

Table S2. Mulliken's atomic charges calculated on the sample (1) of the zwitter-ion form **C** (see Table S3 and S11) by using DFT(wB97XD)/6-31G(d) with PCM for water solvation. The atomic numberings are similar to those shown in Figure S2.

atom	charge in S_0 state at S_0 optimized structure	charge in S_1 state at S_0 optimized structure	charge in S_0 state at S_1 optimized structure	charge in S_1 state at S_1 optimized structure
C1	+0.274795	+0.270821	+0.300060	+0.300870
C2	-0.427820	-0.414423	-0.422612	-0.419838
C3	-0.422946	-0.406911	-0.415522	-0.414398
C4	+0.423734	+0.358669	+0.331606	+0.374039
C5	+0.424842	+0.348184	+0.264211	+0.123771
C6	+0.187455	+0.266395	+0.199348	+0.321344
O7	-0.559827	-0.535140	-0.526032	-0.459294
C8	-0.281703	-0.290191	-0.285258	-0.288731
N9	-0.682590	-0.654404	-0.707294	-0.632452
C10	-0.246126	-0.245204	-0.243492	-0.265380
C11	+0.615717	+0.616479	+0.608590	+0.619750
O12	-0.493018	-0.492270	-0.499622	-0.492263
O13	-0.581503	-0.580367	-0.583152	-0.579033
N14	-0.657974	-0.643761	-0.457718	-0.593042

C15	-0.143776	-0.142230	-0.180137	-0.129970
C16	+0.589913	+0.590998	+0.600837	+0.577914
O17	-0.630404	-0.627456	-0.624629	-0.639348
O18	-0.654112	-0.648000	-0.644001	-0.662582
C19	+0.120858	+0.120849	+0.120684	+0.126944
O20	-0.704795	-0.699088	-0.699202	-0.716056
C21	-0.525337	-0.524264	-0.522694	-0.518042
O22	-0.698954	-0.702256	-0.683273	-0.683721
C23	-0.077301	-0.075103	-0.093543	-0.102771
O24	-0.672339	-0.670384	-0.665842	-0.667208
H25	+0.238914	+0.223451	+0.202084	+0.23881
H26	+0.224273	+0.215093	+0.217861	+0.226507
H27	+0.244323	+0.222732	+0.228538	+0.210966
H28	+0.219749	0.205852	+0.242795	+0.205621
H29	+0.206387	+0.219100	+0.213323	+0.222456
H30	+0.184683	+0.196420	+0.187008	+0.216249
H31	+0.184128	+0.195935	+0.190505	+0.216632
H32	+0.399757	+0.396511	+0.379155	+0.416221
H33	+0.255924	+0.254064	+0.231468	+0.269976
H34	+0.256391	+0.254046	+0.231294	+0.263060
H35	+0.466988	+0.467238	+0.462620	+0.468928
H36	+0.389250	+0.381661	+0.415095	+0.374203
H37	+0.206479	+0.203312	+0.232779	+0.181111
H38	+0.156792	+0.160339	+0.168115	+0.146649
H39	+0.427839	+0.428948	+0.431196	+0.423516
H40	+0.168811	+0.169253	+0.170204	+0.165115
H41	+0.172982	+0.173357	+0.176918	+0.163627
H42	+0.178503	+0.179157	+0.185352	+0.168263
H43	+0.438310	+0.435397	+0.441472	+0.435173
H44	+0.183304	+0.181763	+0.190120	+0.190933
H45	+0.168228	+0.165126	+0.178269	+0.168887

H46	+0.451193	+0.450301	+0.452520	+0.451522

Table S3. Energies of the charge-neutral porphyra-334; (i) Gibbs free energies of the S_0 state calculated with wB97XD/6-31G(d), (ii) Frank-Condon (FC) excitation energies to the S_1 state calculated with time-dependent (TD) DFT(wB97XD/6-311G(d,p)) and (iii) Franck-Condon (FC) excitation energies to the S_1 state calculated with Symmetry Adapted Cluster/Configuration Interaction (SAC-CI) with 6-311G(d,p) basis sets.

form	geometry sample	Gibbs free energy [a.u]	FC [kca/mol] by TDDFT	FC [kcal/mol] by SAC-CI
A	1	-1257.335422	106.093234	97.815904
	2	-1257.329699	106.450696	99.277228
	3	-1257.32955	107.046765	100.223149
	4	-1257.328402	109.018834	103.315753
	5	-1257.330007	106.435914	99.404476
	6	-1257.334439	104.563398	98.096320
	7	-1257.339896	104.065174	94.633203
	8	-1257.337546	104.206489	94.569532
	9	-1257.336615	104.466313	95.033741
	10	-1257.333411	101.559554	92.286354
B	1	-1257.330132	106.093234	97.815904
	2	-1257.330064	106.450696	99.277228
	3	-1257.326564	107.046765	100.223149
	4	-1257.330335	109.018834	103.315753
	5	-1257.326317	106.435914	99.404476
	6	-1257.331457	104.563398	98.096320
	7	-1257.329019	104.065174	94.633203
	8	-1257.327774	104.206489	94.569532
	9	-1257.330939	101.075144	95.033741
	10	-1257.326881	101.559554	92.286354
C	1	-1257.352405	99.767357	86.321282
	2	-1257.349200	97.278985	84.078505
	3	-1257.344001	96.891176	83.028651

	4	-1257.344313	98.881809	84.316098
	5	-1257.341249	93.874188	83.860214
	6	-1257.333061	95.001895	86.163109
	7	-1257.35158	99.766365	83.891738
	8	-1257.349441	97.910637	83.803300
	9	-1257.349906	96.257080	80.842856
	10	-1257.349506	96.912623	82.107151
D	1	-1257.346389	99.938899	87.002329
	2	-1257.341556	97.877845	84.375202
	3	-1257.343067	100.559833	86.410687
	4	-1257.346313	95.435871	79.194834
	5	-1257.344868	99.566015	85.835949
	6	-1257.329019	100.435167	86.553386
	7	-1257.327774	99.831903	85.926070
	8	-1257.34656	99.846478	87.216008
	9	-1257.341191	95.517736	80.513206
	10	-1257.342105	95.549537	80.533430

Table S4. Frank-Condon (FC) excitation energies to the S_1 state of the neutral porphyra-334 calculated with time-dependent (TD) DFT(ωB97XD/6-311G(d,p)) with varying the value of the parameter ω among 0.0, 0.1, 0.2, 0.3, 0.4.

form	geometry sample	ω 0.0	0.1	0.2	0.3	0.4
A	1	99.214160	102.491830	106.093234	109.641780	112.825748
	2	103.436044	103.729508	106.450696	109.927939	113.124941
	3	101.665699	103.261567	107.046765	110.890275	114.223106
	4	103.955987	105.154775	109.018834	113.237174	116.867753
	5	100.739755	102.442151	106.435914	110.535056	114.080522
	6	100.692659	101.349026	104.563398	108.494768	112.044242
	7	101.325801	101.653318	104.065174	107.218349	110.235292
	8	101.692480	101.953803	104.206489	107.181561	110.063585

	9	100.177946	101.214502	104.466313	107.980718	111.135998
	10	95.650518	97.208612	101.559554	105.651133	109.114984
B	1	103.104179	104.517944	106.093234	111.607192	114.839360
	2	104.367470	105.380239	106.450696	113.167910	116.727147
	3	103.076190	104.513556	107.046765	112.038667	115.503255
	4	97.003158	100.496722	109.018834	108.068492	111.043359
	5	103.247622	104.585487	106.435914	111.767082	115.134263
	6	100.043282	104.337217	104.563398	112.007064	115.364953
	7	100.979883	103.251269	104.065174	110.252181	113.431953
	8	102.051504	103.775219	104.206489	110.712381	113.921820
	9	100.926066	103.620630	101.075144	111.988890	115.383926
	10	103.478358	104.422647	101.559554	111.340384	114.685429
C	1	95.025938	97.651422	99.767357	101.540721	103.485149
	2	87.820522	91.020489	97.278985	100.548907	103.040688
	3	86.863834	90.134846	96.891176	100.417346	103.019033
	4	88.677981	93.911277	98.881809	100.998382	103.020359
	5	86.723354	91.294609	93.874188	100.611057	103.117311
	6	88.468566	93.057316	95.001895	101.745159	104.085396
	7	94.511148	97.944587	99.766365	101.521837	103.490911
	8	91.731720	94.393223	97.910637	100.310688	102.568813
	9	86.693756	90.157821	96.257080	99.443816	101.935685
	10	86.508633	90.116157	96.912623	100.312315	102.840254
D	1	91.594732	97.876738	99.938899	101.981257	104.103120
	2	87.055967	90.563591	97.877845	101.397164	103.947507
	3	91.229203	98.990274	100.559833	102.318976	104.295121
	4	89.328063	91.530822	95.435871	98.346123	100.818843
	5	92.073183	98.095143	99.566015	101.380429	103.384466
	6	90.376513	98.258321	100.435167	102.159198	104.118811
	7	91.880094	98.538991	99.831903	101.453261	103.380744
	8	89.932886	97.228612	99.846478	101.931988	104.072364
	9	84.632004	88.706070	95.517736	99.345483	102.096927

10	84.624089	88.705202	95.549537	99.374829	102.123359

Table S5. Component of the S_1 Franck-Condon state at the neutral porphyra-334 calculated with TDDFT(ωB97XD/6-311G(d,p)) level (highest π = highest occupied Kohn-Sham orbital (Figure 2, 5 of the main text), lowest π^* = lowest unoccupied Kohn-Sham orbital (Figure 2, 6 of the main text)).

form	geometry sample	from	to	excitation coefficient
A	1	highest π	lowest π^*	0.69631
	2	highest π	lowest π^*	0.69794
	3	highest π	lowest π^*	0.69482
	4	highest π	lowest π^*	0.69130
	5	highest π	lowest π^*	0.69190
	6	highest π	lowest π^*	0.69756
	7	highest π	lowest π^*	0.69824
	8	highest π	lowest π^*	0.69931
	9	highest π	lowest π^*	0.69608
	10	highest π	lowest π^*	0.69425
B	1	highest π	lowest π^*	0.69788
	2	highest π	lowest π^*	0.67274
	3	highest π	lowest π^*	0.69620
	4	highest π	lowest π^*	0.69719
	5	highest π	lowest π^*	0.69651
	6	highest π	lowest π^*	0.69807
	7	highest π	lowest π^*	0.69813
	8	highest π	lowest π^*	0.69773
	9	highest π	lowest π^*	0.69680
	10	highest π	lowest π^*	0.67656
C	1	highest π	lowest π^*	0.68789
	2	highest π	lowest π^*	0.68602
	3	highest π	lowest π^*	0.68577
	4	highest π	lowest π^*	0.65346

	5	highest π	lowest π^*	0.66263
	6	highest π	lowest π^*	0.66833
	7	highest π	lowest π^*	0.68873
	8	highest π	lowest π^*	0.68365
	9	highest π	lowest π^*	0.68097
	10	highest π	lowest π^*	0.68182
D	1	highest π	lowest π^*	0.69352
	2	highest π	lowest π^*	0.65750
	3	highest π	lowest π^*	0.69385
	4	highest π	lowest π^*	0.67458
	5	highest π	lowest π^*	0.69358
	6	highest π	lowest π^*	0.68708
	7	highest π	lowest π^*	0.69245
	8	highest π	lowest π^*	0.68524
	9	highest π	lowest π^*	0.65455
	10	highestπ	lowestπ^*	0.65414

Table S6. Energies of the first and second spin-triplet states (T_1 and T_2) at the charge-neutral porphyra-334 calculated with Symmetry Adapted Cluster/Configuration Interaction (SAC-CI) with 6-311G(d,p) basis sets.

form	geometry sample	FC [kcal/mol] of T_1	FC [kcal/mol] of T_2
A	1	64.499915	98.797984
	2	67.464533	101.510043
	3	66.104606	99.861513
	4	70.367925	98.756682
	5	66.681212	99.870530
	6	67.033716	103.292854
	7	64.392453	107.056842
	8	64.267695	108.180883
	9	64.016612	102.791702
	10	63.820690	103.675451

B	1	67.326078	98.522180
	2	69.237728	98.114215
	3	68.600196	99.494320
	4	64.576638	101.681590
	5	67.475856	98.839931
	6	67.537404	99.973841
	7	67.186607	102.696577
	8	67.132184	101.321730
	9	67.757333	99.528404
	10	67.317176	99.399334
C	1	60.109256	132.823039
	2	59.371088	126.643596
	3	58.830295	121.968992
	4	58.727699	132.710941
	5	59.594152	132.086139
	6	60.275177	124.999263
	7	59.228712	130.572122
	8	59.615184	129.892666
	9	57.839360	123.291376
	10	60.275177	124.999263
D	1	60.673248	132.440510
	2	59.385339	128.008872
	3	59.656162	128.817652
	4	57.735749	129.134296
	5	59.923434	131.585148
	6	59.935748	130.264148
	7	59.273795	132.924205
	8	60.530987	126.081287
	9	58.568143	124.130619
	10	58.486208	123.994423

Table S7. S_0 optimized structure of geometry sample 7 in form (A) (see Table S1).

C	-2.514290	-1.546995	1.328758
C	-1.050648	-1.962229	1.206114
C	-2.625681	-0.080383	1.752709
C	-0.225986	-0.968308	0.442098
C	-1.835361	0.850894	0.863360
C	-0.616074	0.327967	0.292792
O	0.192820	1.166937	-0.450023
C	1.009478	2.011016	0.359594
N	0.924402	-1.401399	-0.157641
C	1.702029	-2.507394	0.331403
C	2.355363	-2.238281	1.680912
O	2.175090	-1.253443	2.358744
O	3.154119	-3.250321	2.034339
N	-2.139736	2.080861	0.625027
C	-3.327857	2.720064	1.136398
C	-3.523380	3.991206	0.299234
O	-2.616554	4.170307	-0.642166
O	-4.422725	4.789266	0.505247
C	-3.253507	3.115865	2.637659
O	-4.497827	3.637501	3.059611
C	-2.100018	4.068292	2.937512
O	-3.088730	-1.751493	0.045273
C	-3.236955	-2.452696	2.329848
O	-2.664531	-2.278835	3.609964
H	-1.023696	-2.935318	0.704495
H	-0.629086	-2.096451	2.208921
H	-3.682689	0.208644	1.776933
H	-2.253752	0.013992	2.779651
H	1.672117	2.551028	-0.319548
H	0.395489	2.726247	0.916349
H	1.605609	1.413382	1.059704
H	1.455648	-0.653222	-0.584441
H	2.485137	-2.740369	-0.394382
H	1.094387	-3.412659	0.425581
H	3.535166	-3.043154	2.904227
H	-2.004431	3.384207	-0.524843
H	-4.238961	2.118643	1.009211
H	-3.107442	2.192917	3.207100
H	-4.748811	4.302393	2.394456
H	-2.231966	5.022242	2.413872
H	-2.063010	4.273483	4.010815
H	-1.144052	3.632429	2.631349
H	-3.994374	-1.413639	0.060483

H	-3.145230	-3.490577	1.980301
H	-4.305824	-2.188388	2.331884
H	-3.107518	-2.880661	4.219863

Table S8. S_1 optimized structure of geometry sample 7 in form (A) (see Table S1).

C	-2.324524	-1.062703	1.868700
C	-1.169927	-1.526765	0.961621
C	-1.898740	0.086513	2.826781
C	-0.031197	-0.571040	0.738528
C	-1.196147	1.187251	2.066428
C	0.009122	0.658209	1.416839
O	1.180397	1.280244	1.406018
C	1.329579	2.477007	2.184536
N	1.052424	-0.989741	0.069434
C	1.306456	-2.333837	-0.382675
C	1.782729	-3.248930	0.738366
O	1.793847	-2.961684	1.911183
O	2.170700	-4.426120	0.245101
N	-1.801082	1.984308	1.135418
C	-3.175237	2.367955	1.319427
C	-3.821222	2.405945	-0.068962
O	-3.021809	1.987481	-1.027960
O	-4.957627	2.808498	-0.279822
C	-3.337404	3.745725	2.010883
O	-4.710011	4.006730	2.260740
C	-2.680409	4.881373	1.233785
O	-3.367232	-0.655368	0.987050
C	-2.844848	-2.270270	2.659651
O	-1.820481	-2.751216	3.506119
H	-1.600300	-1.842878	0.005031
H	-0.727015	-2.415141	1.426975
H	-2.790825	0.439745	3.360277
H	-1.228743	-0.337406	3.583395
H	2.272055	2.913364	1.857207
H	0.495241	3.151528	1.994578
H	1.378842	2.225370	3.245416
H	1.822608	-0.335762	0.016377
H	2.067074	-2.303415	-1.164812
H	0.410168	-2.771661	-0.831178
H	2.445306	-4.990087	0.987824
H	-2.176210	1.777261	-0.497989
H	-3.779838	1.670611	1.915182
H	-2.856853	3.655710	2.991565
H	-5.163033	3.812207	1.421007
H	-3.183686	5.032106	0.271032
H	-2.746916	5.814767	1.800452
H	-1.627926	4.652468	1.042911
H	-4.136014	-0.419997	1.523906

H	-3.170963	-3.038255	1.944302
H	-3.724115	-1.952918	3.242569
H	-2.110065	-3.593615	3.875535

Table S9. S_0 optimized structure of geometry sample 6 in form (B) (see Table S1).

C	-2.816682	0.368011	2.837285
C	-1.811488	-0.548587	3.535417
C	-2.090509	1.539153	2.174582
C	-0.660653	-0.975029	2.643726
C	-1.025207	1.035389	1.240440
C	-0.375219	-0.129646	1.488130
O	0.617163	-0.509680	0.607459
C	0.208155	-1.549404	-0.278794
N	0.071069	-2.012222	2.835823
C	-0.215901	-2.853557	3.969496
C	0.815582	-3.955350	4.115973
O	1.769459	-4.159908	3.403732
O	0.527809	-4.717975	5.185175
N	-0.653572	1.804525	0.157446
C	-1.591239	2.601825	-0.596961
C	-2.774097	1.777944	-1.110667
O	-3.563739	2.494374	-1.919226
O	-3.008162	0.623696	-0.826254
C	-0.843205	3.341170	-1.742515
O	-1.583722	4.450933	-2.199408
C	-0.431573	2.424022	-2.892597
O	-3.562707	-0.366488	1.866256
C	-3.874361	0.866581	3.826045
O	-4.880662	1.590828	3.153008
H	-2.346634	-1.430840	3.900411
H	-1.398227	-0.038873	4.417796
H	-2.831206	2.153921	1.658067
H	-1.633286	2.177091	2.941067
H	1.032018	-1.706615	-0.977723
H	0.012981	-2.472373	0.275346
H	-0.691097	-1.250670	-0.831646
H	0.038913	1.323744	-0.405777
H	-1.194953	-3.350338	3.890610
H	-0.236575	-2.307123	4.924277
H	1.208179	-5.408919	5.241110
H	-4.297767	1.930165	-2.218546
H	-2.010019	3.391944	0.036249
H	0.051895	3.759792	-1.273468
H	-2.393127	4.110531	-2.607343
H	0.159974	2.993300	-3.613735
H	0.174453	1.577326	-2.553613
H	-1.310884	2.026332	-3.411638
H	-3.155451	-0.247207	0.992782
H	-3.424357	1.531318	4.568838

H	-4.296699	-0.002729	4.353746
H	-5.089802	1.042356	2.379867

Table S10. S_1 optimized structure of geometry sample 6 in form (B) (see Table S1).

C	-2.889151	0.171454	2.491143
C	-2.045167	-0.934795	3.113629
C	-1.960506	1.385657	2.173175
C	-0.685912	-1.156322	2.466162
C	-0.986954	0.958995	1.140905
C	-0.309284	-0.282131	1.389681
O	0.700864	-0.506440	0.527972
C	1.114735	-1.841491	0.222495
N	0.216650	-2.012411	2.929873
C	-0.085240	-2.699568	4.140419
C	0.910812	-3.809940	4.416656
O	1.767202	-4.225342	3.671054
O	0.710867	-4.327982	5.643564
N	-1.116140	1.340002	-0.172863
C	-1.588274	2.630139	-0.604227
C	-3.101595	2.626987	-0.818670
O	-3.524792	3.775998	-1.350549
O	-3.857800	1.719817	-0.546046
C	-0.811817	3.086842	-1.877709
O	-0.939116	4.473929	-2.079456
C	-1.183838	2.285367	-3.122672
O	-3.492398	-0.340036	1.308647
C	-4.021292	0.599436	3.435185
O	-4.919224	1.472041	2.783521
H	-2.633761	-1.861367	3.075142
H	-1.901121	-0.709676	4.180195
H	-2.567398	2.242743	1.871367
H	-1.445273	1.644803	3.107701
H	1.759426	-1.748430	-0.651631
H	1.638063	-2.279447	1.070704
H	0.239470	-2.453738	-0.014221
H	-0.475816	0.861415	-0.797016
H	-1.082060	-3.184734	4.157006
H	-0.088665	-2.049612	5.037636
H	1.350519	-5.049582	5.759442
H	-4.488540	3.727452	-1.477154
H	-1.380638	3.386422	0.167300
H	0.245257	2.928764	-1.643469
H	-1.866955	4.656043	-2.287382
H	-0.537708	2.583421	-3.951924
H	-1.066618	1.207895	-2.967885
H	-2.222901	2.475074	-3.414275
H	-3.450791	0.325074	0.598489
H	-3.620365	1.134184	4.301537

H	-4.538174	-0.303072	3.797132
H	-5.153709	1.018900	1.959667

Table S11. S_0 optimized structure of geometry sample 1 in form (C) (see Table S1).

C	-0.501877	2.215336	-0.467783
C	-1.796846	1.446439	-0.786358
C	0.708755	1.408823	-0.931807
C	-1.750706	0.018256	-0.334794
C	0.687750	-0.005193	-0.428549
C	-0.536610	-0.628678	-0.143821
O	-0.537258	-1.941466	0.276628
C	-0.445371	-2.071249	1.701238
N	-2.879652	-0.652455	-0.132856
C	-4.220382	-0.142082	-0.294187
C	-5.188591	-1.285569	-0.075739
O	-4.850769	-2.415225	0.194613
O	-6.446898	-0.882712	-0.216358
N	1.800558	-0.695571	-0.301054
C	3.166391	-0.289939	-0.569879
C	3.995533	-1.594684	-0.783027
O	3.380695	-2.676243	-0.688508
O	5.221564	-1.412022	-0.997212
C	3.789415	0.544882	0.580090
O	5.061848	0.994490	0.170015
C	3.850247	-0.226864	1.896579
O	-0.486062	3.426731	-1.191760
C	-0.410287	2.552140	1.025733
O	-1.480710	3.444183	1.288050
H	-1.950308	1.465279	-1.872476
H	-2.644644	1.965936	-0.330662
H	0.699769	1.373060	-2.029236
H	1.627906	1.921243	-0.641409
H	-0.461328	-3.140059	1.915421
H	0.488389	-1.635031	2.072303
H	-1.294085	-1.581936	2.191210
H	-2.811430	-1.641004	0.092924
H	-4.382408	0.270129	-1.295956
H	-4.446265	0.645910	0.432811
H	-7.031440	-1.644903	-0.065384
H	1.739716	-1.705685	-0.144967
H	3.213265	0.307829	-1.486265
H	3.174270	1.439902	0.735161
H	5.453935	0.208415	-0.275639
H	2.853307	-0.550125	2.215346
H	4.490232	-1.110165	1.797614
H	4.269158	0.414179	2.677465
H	-1.020990	4.043702	-0.665710
H	0.558198	3.032013	1.213747

H	-0.480634	1.648392	1.644222
H	-1.296983	3.914876	2.109244

Table S12. S_1 optimized structure of geometry sample 1 in form (C) (see Table S1).

C	0.330579	1.653745	-0.692098
C	0.827324	0.942806	0.604988
C	-0.580071	0.699532	-1.529828
C	1.377755	-0.402040	0.253531
C	-0.787814	-0.629063	-0.840326
C	0.491867	-1.228120	-0.475654
O	0.955156	-2.380992	-0.921899
C	0.117905	-3.160594	-1.792117
N	2.643011	-0.733558	0.434115
C	3.677991	0.130736	0.965193
C	5.011741	-0.554162	0.759083
O	5.134961	-1.649273	0.260349
O	6.010765	0.200801	1.198860
N	-1.753610	-0.749664	0.132562
C	-2.856153	0.156645	0.355100
C	-3.395854	-0.085126	1.794878
O	-2.751960	-0.868612	2.523086
O	-4.449124	0.544526	2.086194
C	-3.977679	0.000113	-0.697335
O	-4.947282	1.009457	-0.495604
C	-4.597814	-1.395805	-0.682680
O	-0.425836	2.788715	-0.325850
C	1.531222	2.099547	-1.527696
O	2.306005	2.967887	-0.717498
H	-0.033412	0.812548	1.267091
H	1.553599	1.572556	1.118262
H	-1.525179	1.214551	-1.715386
H	-0.120136	0.526342	-2.509216
H	0.642854	-4.104293	-1.924000
H	-0.856822	-3.321336	-1.329330
H	0.001575	-2.648927	-2.748683
H	2.963903	-1.641800	0.105239
H	3.531199	0.312874	2.034267
H	3.680390	1.097889	0.450633
H	6.845347	-0.276458	1.052823
H	-1.618005	-1.369919	0.925815
H	-2.508694	1.198686	0.313635
H	-3.539734	0.172931	-1.689351
H	-5.047490	1.023186	0.485064
H	-3.836085	-2.166039	-0.844213
H	-5.087931	-1.583430	0.279163
H	-5.350865	-1.478068	-1.472086
H	0.214413	3.458464	-0.038331
H	1.156783	2.615203	-2.420596

H	2.117849	1.228369	-1.854031
H	2.903157	3.469858	-1.284859

Table S13. S_0 optimized structure of geometry sample 8 in form (D) (see Table S1).

C	-0.112953	0.956967	-0.924301
C	-1.078571	2.092922	-0.595213
C	-0.756822	-0.400347	-0.588491
C	-1.659662	1.979366	0.781917
C	-1.335937	-0.440084	0.793371
C	-1.719848	0.729437	1.427849
O	-2.262424	0.657790	2.693211
C	-1.294413	0.867062	3.729112
N	-2.149433	3.036660	1.379030
C	-2.208514	4.408171	0.912344
C	-2.936258	5.249606	2.005949
O	-3.306703	4.608289	3.021186
O	-3.063661	6.459343	1.746309
N	-1.511497	-1.597860	1.436250
C	-1.270958	-2.947261	0.964422
C	-2.568623	-3.494816	0.363563
O	-3.281158	-4.314568	0.902266
O	-2.840372	-2.936919	-0.813579
C	-0.809059	-3.813484	2.150703
O	-1.746854	-3.703427	3.208300
C	0.547430	-3.376403	2.672672
O	0.135446	1.024634	-2.312863
C	1.224936	1.128158	-0.193745
O	2.083416	0.126904	-0.715157
H	-1.905107	2.064403	-1.317430
H	-0.582492	3.059683	-0.721888
H	-1.555558	-0.600596	-1.311271
H	-0.004146	-1.183066	-0.714315
H	-0.864927	1.872548	3.664139
H	-1.825306	0.755266	4.674730
H	-0.490861	0.125167	3.665286
H	-2.612025	2.957816	2.292054
H	-2.756562	4.477975	-0.032754
H	-1.202740	4.811167	0.754847
H	-1.972589	-1.549514	2.340900
H	-0.506806	-2.945104	0.184889
H	-0.749786	-4.850439	1.795682
H	-2.560023	-4.126493	2.890279
H	0.515514	-2.339068	3.019792
H	0.840474	-4.013663	3.510640
H	1.305736	-3.458537	1.888448
H	0.971350	0.548230	-2.445166
H	1.103450	1.025445	0.891947
H	1.612592	2.131064	-0.410418

H	2.995760	0.371028	-0.521163
H	-3.695000	-3.278214	-1.129114

Table S14. S_1 optimized structure of geometry sample 8 in form (D) (see Table S1).

C	0.029121	1.019209	-0.306906
C	0.034896	2.173381	0.745641
C	-1.301248	0.212117	-0.223653
C	-1.207554	2.170330	1.607831
C	-1.526028	-0.217035	1.189000
C	-1.485025	0.835137	2.132875
O	-1.520375	0.504335	3.410289
C	-1.290352	1.528331	4.392244
N	-2.335398	2.805436	1.136309
C	-2.326929	4.005497	0.326150
C	-3.738629	4.658516	0.364147
O	-4.564728	4.137864	1.155352
O	-3.891412	5.640953	-0.389341
N	-1.558203	-1.480212	1.583525
C	-1.311316	-2.672170	0.785224
C	-2.650499	-3.267435	0.347508
O	-3.087555	-4.325398	0.742400
O	-3.279416	-2.470279	-0.510444
C	-0.510996	-3.669385	1.641493
O	-1.193481	-3.898898	2.861490
C	0.875294	-3.140486	1.965190
O	0.135666	1.586536	-1.595987
C	1.216311	0.084913	-0.068677
O	1.135771	-0.957736	-1.028214
H	0.132654	3.117785	0.205540
H	0.921881	2.080702	1.382910
H	-2.114067	0.881944	-0.516750
H	-1.285368	-0.621829	-0.922853
H	-1.959778	2.372451	4.221974
H	-1.499296	1.056416	5.349955
H	-0.250615	1.855592	4.345092
H	-3.202637	2.761508	1.667367
H	-2.063204	3.771760	-0.711518
H	-1.595866	4.735378	0.696612
H	-1.684743	-1.667340	2.576272
H	-0.729437	-2.405563	-0.100724
H	-0.427094	-4.597259	1.062900
H	-1.996363	-4.394011	2.636371
H	0.814601	-2.241760	2.588003
H	1.441472	-3.897604	2.512533
H	1.413394	-2.893388	1.045291
H	0.373395	0.859095	-2.191861
H	1.191765	-0.316668	0.954628
H	2.140081	0.664044	-0.186964

H	2.006902	-1.360567	-1.124720
H	-4.137133	-2.868969	-0.738283